

# Investigating the electronic structure, magnetic, and optical properties of the KCrS half Heusler compound from first principles

Rabab A. Saleh, Jabbar M. AL-Zyadi\* 

Department of Physics, College of Education for Pure Sciences, University of Basrah, Basrah, Iraq.

## ARTICLE INFO

Received 21 March 2024  
Accepted 23 May 2024  
Published 30 June 2024

## Keywords :

KCrS half-Heusler Compound,  
DFT, Half-metallic, magnetic  
moment.

**Citation:** R. A. Saleh, J. M. AL-Zyadi, J. Basrah Res. (Sci.) 50(1), 125 (2024).  
[DOI:https://doi.org/10.56714/bjrs.50.1.11](https://doi.org/10.56714/bjrs.50.1.11)

## ABSTRACT

Using first principles calculations, which were conducted within the framework of Density Functional Theory (DFT) and General Gradient Approximation (GGA), which were implemented using the WIEN2k code program, in order to calculate the structural, electronic, magnetic, and optical properties of the KCrS compound. The results show that the compound achieves the property of half-metal at the equilibrium constant (6.63), where it behaves like a metal in the spin up channel while it behaves like a semiconductor in the spin down channel. The total magnetic moment of KCrS is 5, and the energy gap of this compound is (3,29). In addition, the compound showed distinctive optical properties, which makes it a strong choice for optical and optoelectronic uses. High reflection of light appears in UV, and this is important in laser technology and stimulated emission.

## 1. Introduction

A new class of materials, which is called half-metallic material, like Heusler alloys, recently ensured that they have attracted considerable attentions from different sectors in electronics industry for their interesting applications. The fact that these materials contain both metallic and non-metallic properties is their strength. This makes them suitable for application where there is a need to combine electricity conductivity and good performance in terms of magnetic and thermoelectric properties. [1-7]. A sub-class of materials that have been paying continuous attention by scientists in the last decades is half-metallic compounds, for they have very special electronic and magnetic characteristics. Thus, the materials demonstrate the metallic behavior within one spin channel while being semiconducting at the same time thus favoring the charge carriers in the spin channel opposing the direction of spin at the Fermi energy surface. These are the electric spin due to the angular momentum of electrons. Due to this trait they are highly suitable for applications where the spin of electron is manipulated to perform logical operations [8-11]. When half-metallic response was revealed in the system of half-Heuslers alloys NiMnSb and PtMnSb by De Groot and co-workers in 1983, the researching of this area completely started. This was the first instance where new class of materials primarily constituting half-metals got discovered. Since then, over the years, other half-metallic materials have been studied resulting in an ongoing work with the aim of understanding their properties and in the development of better materials with improved performance [12,13]. Although

\*Corresponding author email : [jabbar.khalaf@uobasrah.edu.iq](mailto:jabbar.khalaf@uobasrah.edu.iq)



they demonstrate a great promise, the study of half-metallic systems is an emerging field of investigation which is still in the stage of development, and the research community knows much more about half-metallic systems than that. This study work to study the behavior of half-metals materials, the properties and to identify ways of improving their applicability for spintronics devices and other technologies [14,15].

## 2. Computational method

Considering Density Functional Theory (DFT), realized using the WEN2K and CASTEP software tools, we have obtained the first-principles calculations. However, for this computational study, the Perdew-Burke-Ernzerhof (PBE) exchange-correlation functional was the one selected and GGA, which was used for such calculations [16-19]. We use the generalized gradient approximation (GGA) not only for the optimization of  $R_{MT} \times K_{Max}$ , K-Point, and lattice constant, but also for the range of Fermi velocity in our study [20]. Now, we have the energy optimization results. For the determination of the smallest radius of the muffin-tin sphere we used  $R_{MT} = 8$ , where  $R_{MT}$  is the smallest radius of the muffin-tin sphere, and  $K_{Max}$  stands for the maximum reciprocal lattice vector used for expanding the plane wave function. Here, the MT spheres' (MTs) radii ( $R_{MT}$ ) remain uniform and are kept at 2.5 a.u., for each atoms (K, Cr, and S). This is in both bulk substrate and at molecular interface. Additionally, the angular momentum expansion within the MTs is established at  $l_{max} = 10$ . The self-consistent field calculation iterations exhibit a convergence criterion of less than  $10^{-5}$  Ry per formula unit. These adjustments contribute to refining the accuracy and reliability of our computational model, ensuring a comprehensive exploration of the system's electronic structure and properties.

## 3. Results and discussion

### 3.1 Bulk properties

Heusler's triple alloys, including half-Heusler's structures, consist of three interlocking FCC sub-lattices, each occupied by different types of atoms. The space-group lattice for this configuration is designated as No. 216, where K, Cr, and S atoms are positioned at coordinates (0, 0, 0), (0.25, 0.25, 0.25), and (0.5, 0.5, 0.5), respectively [21]. The equilibrium lattice constant for this compound is determined to be 6.63 Å (see Fig. 1).

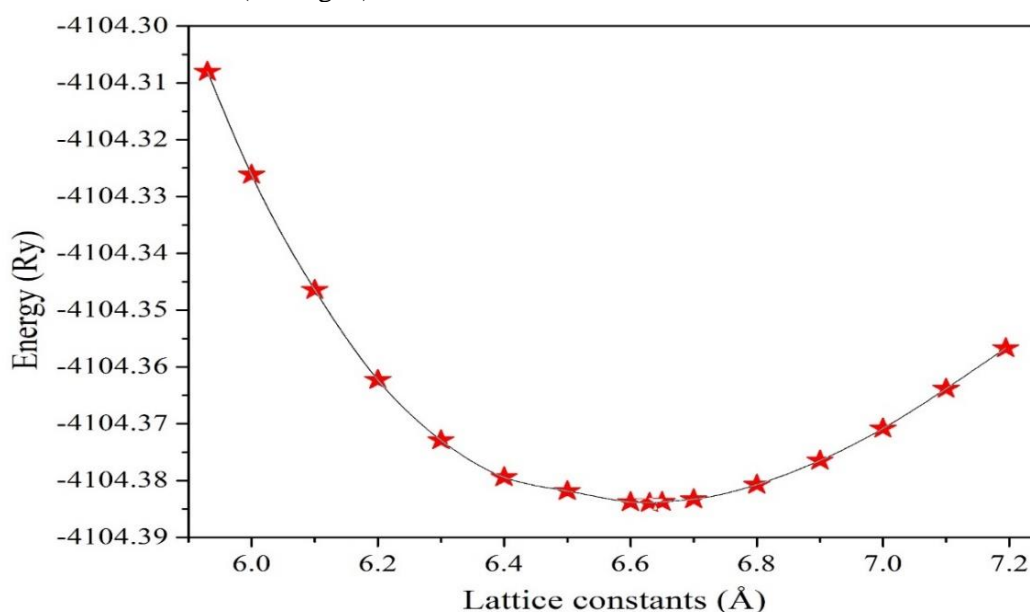


**Fig.1.** Correlation between Total Energies per Unit Cell and Lattice Parameters in KCrS.

It is noteworthy that an affinity lattice constant, consistent with a prior study [22], has been identified, resulting in minimal alterations in the energy gap. This information underscores the significance of the material's electronic properties within specific lattice constant parameters. The relationship between half-metallic (HM) nature and lattice constants is of paramount importance from both theoretical and practical perspectives. In Fig. 2, we present a plot detailing, which depicts the energy state diagram for KCrS in spin-down states along with the lattice constants of the material. Conduction band minimum (CBM) and valence band maximum (VBM) curves' behaviour signifies the energy barrier restricting the formation [23]. What is more, the calculated magnetic properties indicate that the KCrS compound possesses half-metallic ferromagnetism in the framework of lattice constants that is beyond 6.1 to 7.2 Å. It points to the importance mechanism of lattice constants in constructing half-metallic character of the entire materials. Such perspectives are critical in both theoretical progress, which is an interesting subject of study, and practical implementations, which is an absolute prerequisite for construction of a pure electronic and magnetic materials.

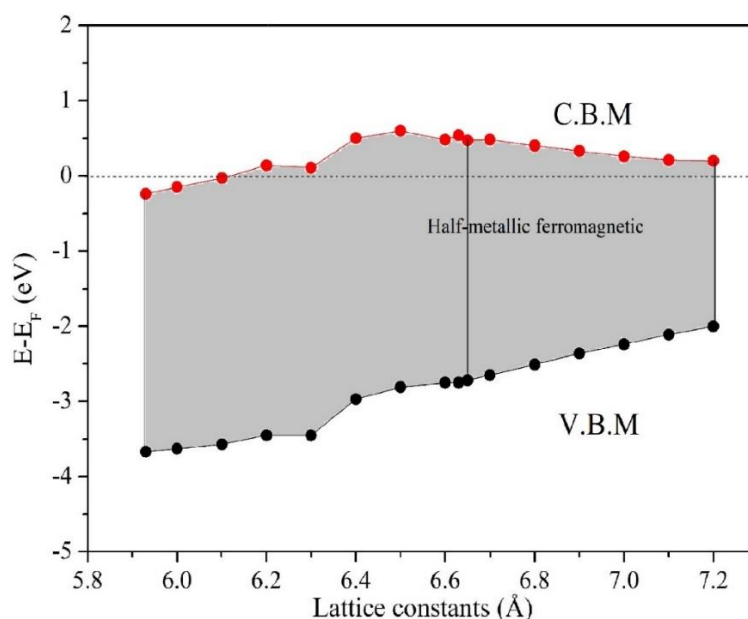


**Fig.2.** Along the width of the lattice, the band gap in half-Heusler KCrS compound changes.

The substance with the bulk material KCrS exhibits the plain intensive 100% spin polarization. That feature is a distinguishing mark for the substance which reflects its magnetic properties. In connection with this, the total magnetic moment ( $M_t$ ), just like recently formulated Slater-Pauling rule, is dependent on the total number of valence electrons ( $Z_t$ ). In the KCrS unit cell, EITHER we will have a total of 13 valence electrons which fill  $K(3s^23p^64s^1)$ ,  $Cr(4s^14p^03d^5)$ , and  $S(3s^23p^4)$ . Consequently, the resultant total magnetic moment clusters equals  $5\mu_B$ , indicating follows the Slater-Pauling curve [24]. The discovery shows that KCrS has a special magnetic property which gives rise to the bright prospects for carry-on researches to pinpoint the field of spintronics or like fields. The magnetic moment of the atomic three of K, Cr, and S is given as  $0.112\mu_B$ ,  $4.304\mu_B$ , and  $-0.048\mu_B$ , respectively. KCrS, the most considerable part of spin the total atomic magnetic moment being caused by Cr atom can be noticed in Fig. 3. This conclusion underlines the important function of a specific Cr atom, which underlies the magnetic behavior of the compound KCrS that may be derived only from the knowledge of the electronic structure of each separate component.

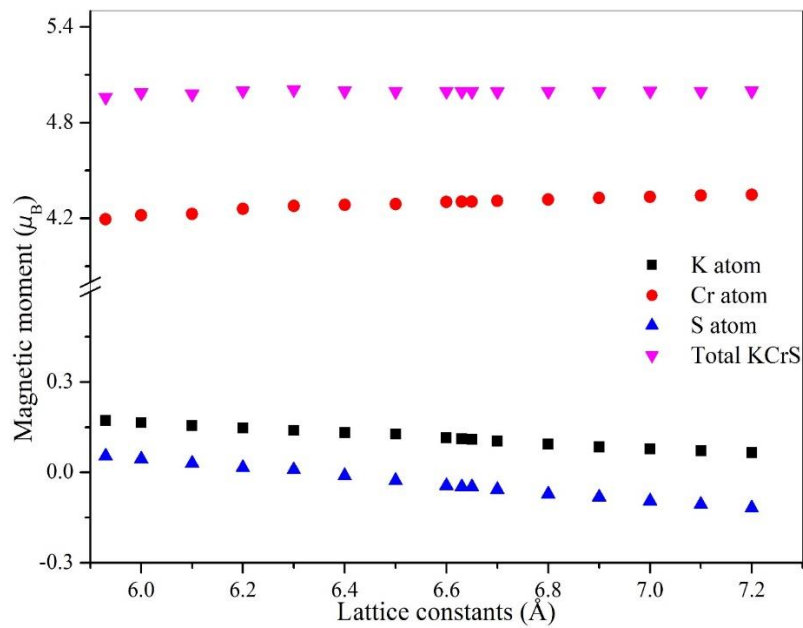


**Fig.3.** Change of total magnetic moment in KCrS compound with lattice parameters.

The DOS was plotted both for the total and bulk densities of states and is shown in Figure 4 shows that the analyzed the electronic structure of the equilibrium state of the half-Heusler alloy of the KCrS. The main point of half-Heusler alloy KCrS is that this KCrS compound exhibits semiconducting properties in the spin-down band channel by having a band gap at Fermi level. Thence, under the spin-up process the conductor shows a metallic nature. These main properties are repaired by Cr-d effect. Obviously, as KCrS alloy has a prominent high energy gap near the Fermi level, and has only a measurement of 3.29 eV. This feature is a crucial factor that transforms our knowledge of the material behaviour in electronics. This complete characterization gives a good overview of the emergent electronic properties that differentiates these materials [25].

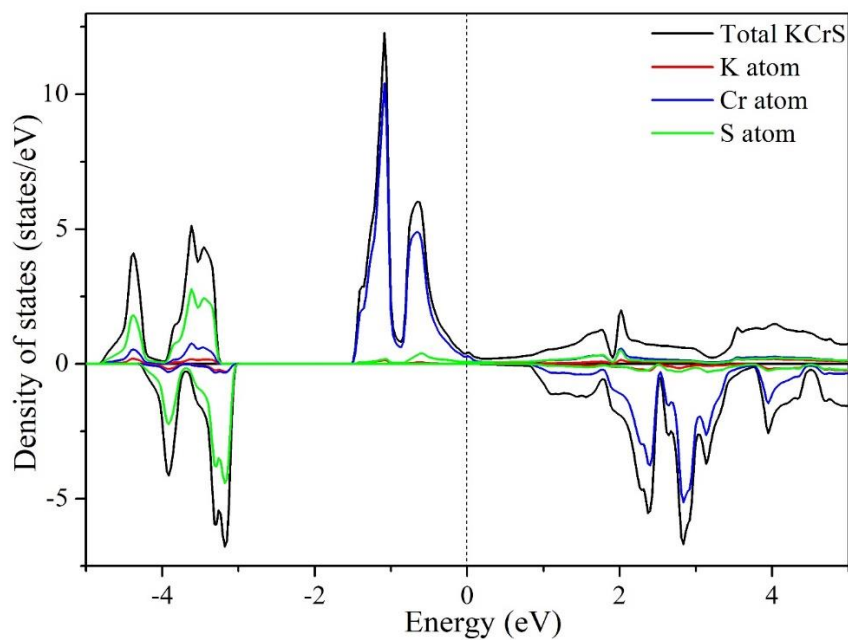


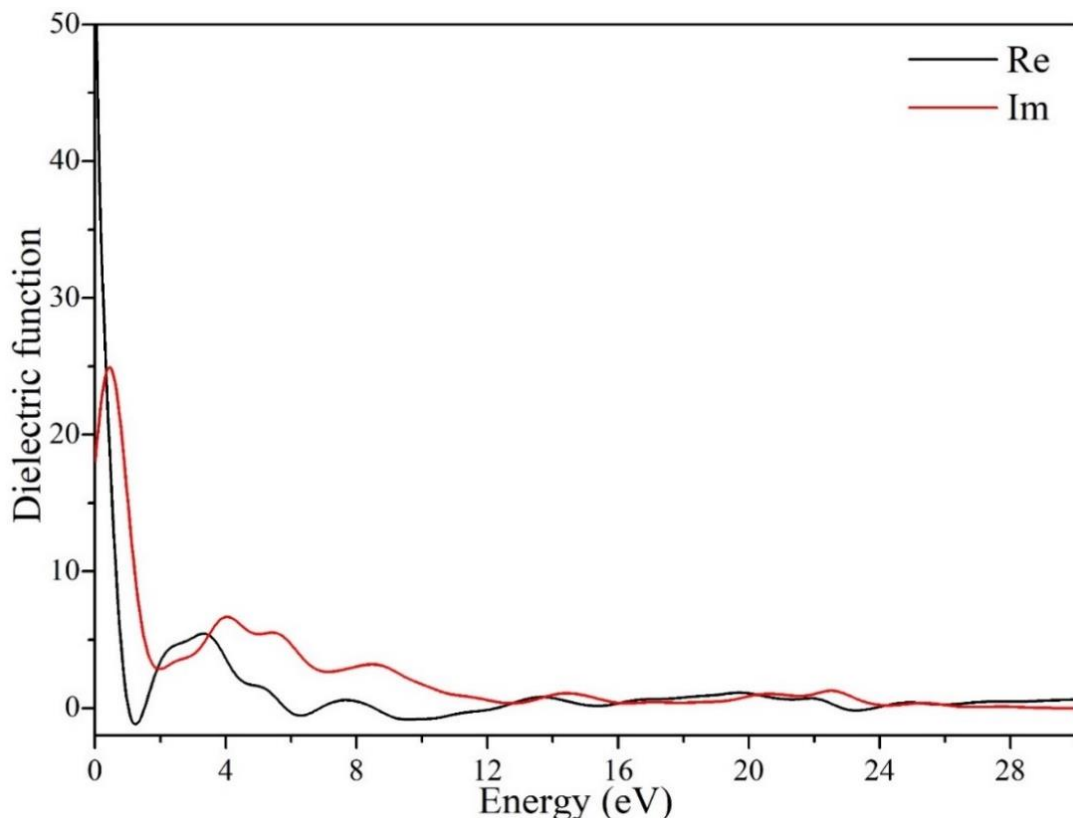
**Fig.4.** Total and Partial Density of States in a Half-Heusler KCrS Compound.

### 3.2 Optical properties

Determining half-Heusler (HH) KCrS possible optoelectronic uses requires examining its optical characteristics. In order to analyses optical properties in the energy range of 0 to 30 eV, this work uses the Generalized Gradient Approximation (GGA) energy exchange correlation functional. The Kramer–Kronig relation is used in the investigation of optical characteristics, with an emphasis on energy absorption or dissipation. This relationship may be stated as follows in equation form:

$$\varepsilon(\omega)=\varepsilon_1(\omega)+i\varepsilon_2(\omega)$$

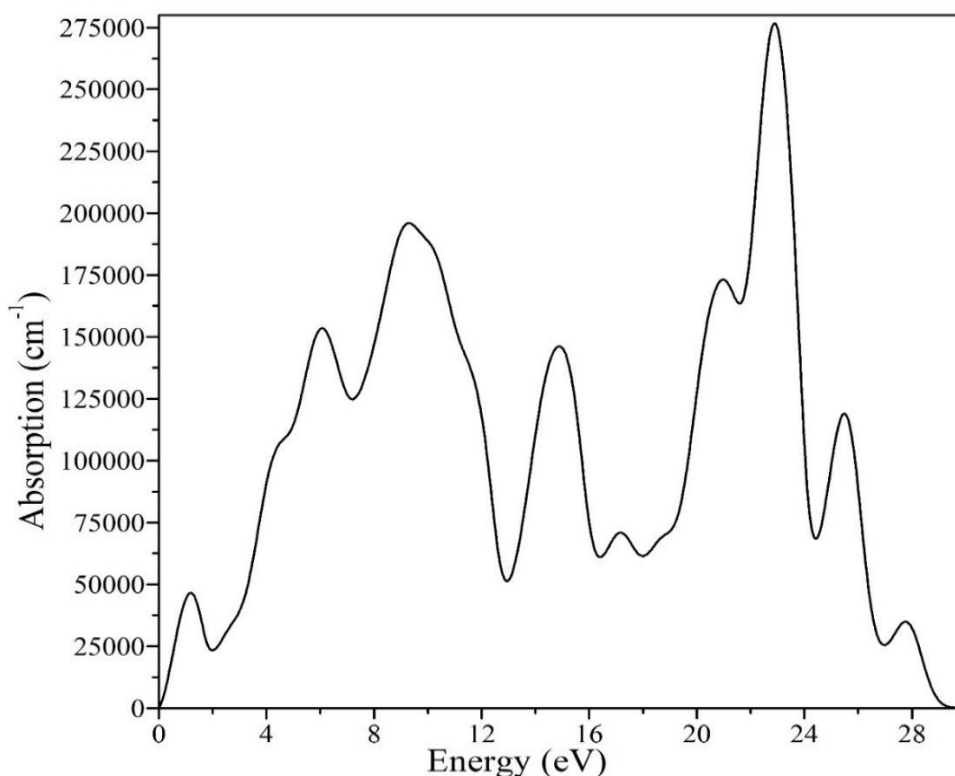
Here,  $\varepsilon_1(\omega)$  signifies the real part of the dielectric function, representing the dispersion relation of electromagnetic waves. On the other hand,  $\varepsilon_2(\omega)$  is the imaginary part of the dielectric function, reflecting the disparity between the wave functions of occupied and unoccupied levels, as computed through the momentum matrix element [26]. Fig. 5 illustrates the real and imaginary parts of the dielectric functions. The zero value of the energy of the incident photon corresponds to a real dielectric function of 50, while the imaginary dielectric function corresponds to it 25. The highest peak in the real part of the dielectric function occurs at an energy value of 3.31 eV. The image makes it clear that the dielectric function's real component displays both positive and negative values, reflecting the material's interaction with radiation or light. Positive numbers, which indicate that the material scatters light more or changes its direction based on its optical qualities, indicate an increase in refraction or light scattering. Conversely, negative values suggest that the substance absorbs light in this range and hence gains energy from it. The image shows that, with regard to the imaginary component of the dielectric function, the greatest peak is nearly zero in relation to the other peaks. This implies a high probability of low-energy optical conductivity, indicating the metallic property of the material. The maximum value, at 24.93 for an energy of 1.2 eV.



**Fig.5.** illustrates the imaginary and real components of the dielectric function for the half-Heusler compound KCrS.

From Fig. 6 it can be seen that as the energy of the incident light increases, the absorption coefficient increases, and there are 7 peaks. The first peak begins in the infrared range, while the other six peaks

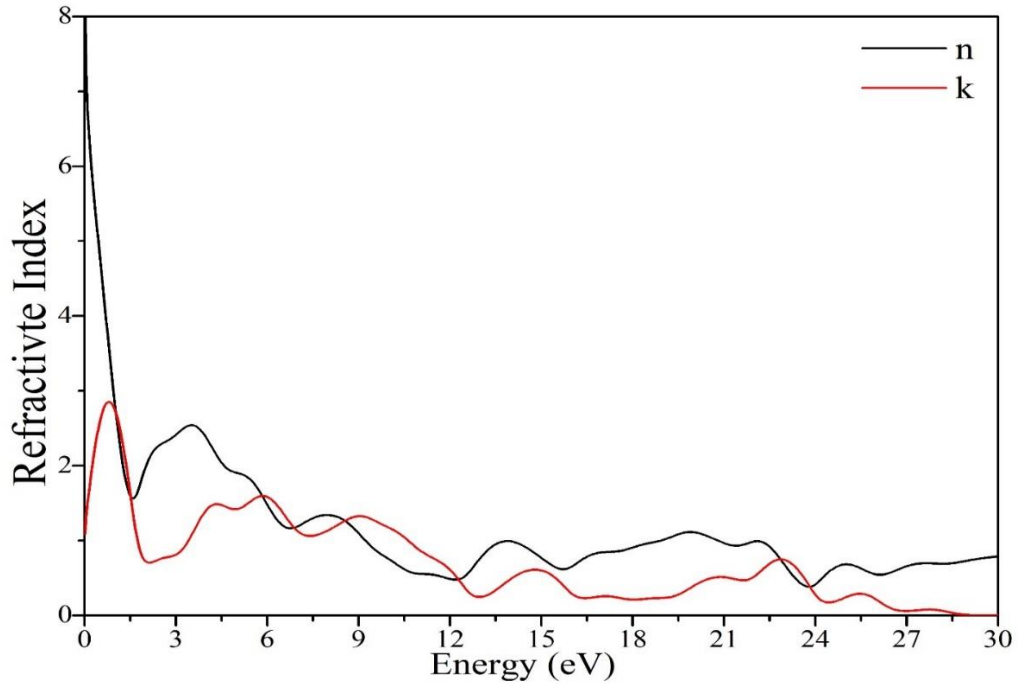
occur in the ultraviolet range, and the highest peak occurs at energy 24.4 eV. After that, the absorption goes to zero at energies older than 29 eV. A critical range for examining light absorption can be leveraged in the manufacturing of solar cells [26].



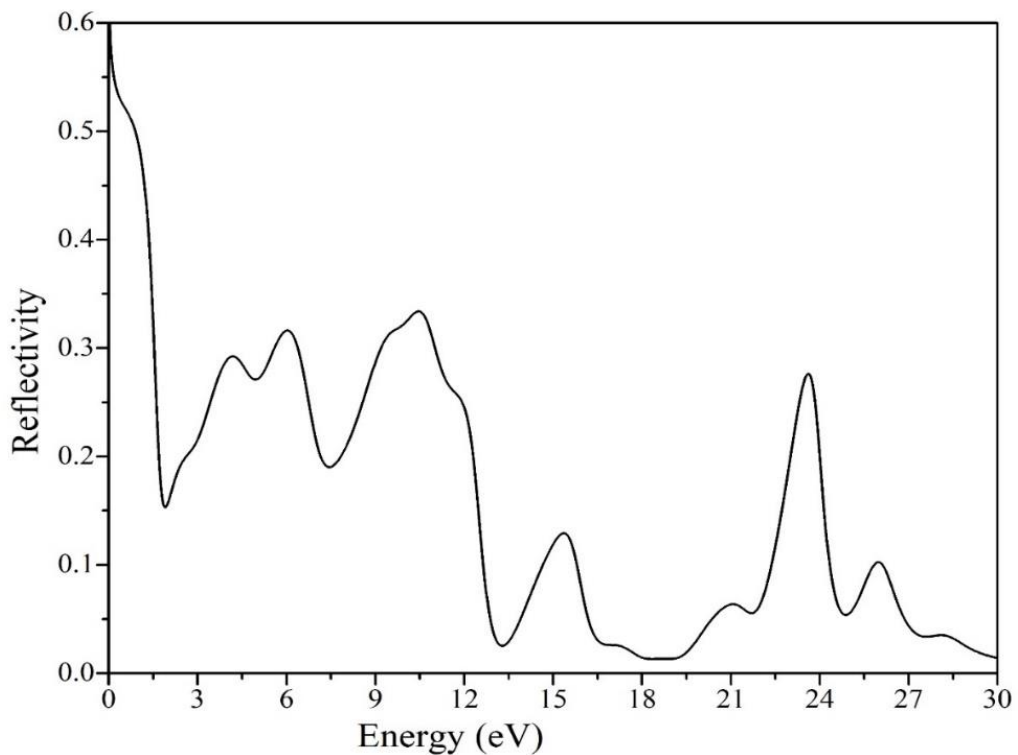
**Fig. 6.** showcases the absorption coefficient for the half-Heusler compound KCrS.

Fig. 7 illustrates the refractive index ( $n$ ) and extinction coefficient ( $k$ ) for the KCrS compound as a function of photon energy. The refractive index and extinction coefficient values at zero energy for this compound are 7.33 and 1.08, respectively. the maximum value of the refractive index is 2.54 at 3.54 eV, whereas the maximum value of the extinction coefficient is 2.85 at 0.79 eV. As photon energy increases, it is observed that the refractive index decreases towards zero and stabilizes at values close to zero. In contrast, a distinct peak in the refractive index is prominent in the infrared region. The high value of the refractive index indicates that, during light transmission, incident photons interact with more valence electrons, leading to high polarization and consequently a reduction in the speed of light [27]. In summary, the graphical representation underscores the dynamic behavior of refractive index and extinction coefficient with changing photon energy, elucidating the material's optical response and its impact on light transmission characteristics.

Fig. 8 describes the optical reflectance as a function of photon energy. It is evident from the figure that the static reflectance (at zero energy) for the KCrS compound is approximately 0.58. Several notable peaks in optical reflectance occur at specific photon energies (6.04 eV, 4.307 eV, 10.47 eV, 15.37 eV, 23.62 eV, and 25.97 eV). The highest peak in reflectance is observed at a value of 0.334 at an energy of 10.47 eV. The appearance of multiple peaks in the reflectance curve is a result of electronic transitions, where the increase in peak values signifies an augmentation in electronic transitions between valence and conduction bands. The height of these peaks depends on the energy required for these electronic transitions to occur [28].

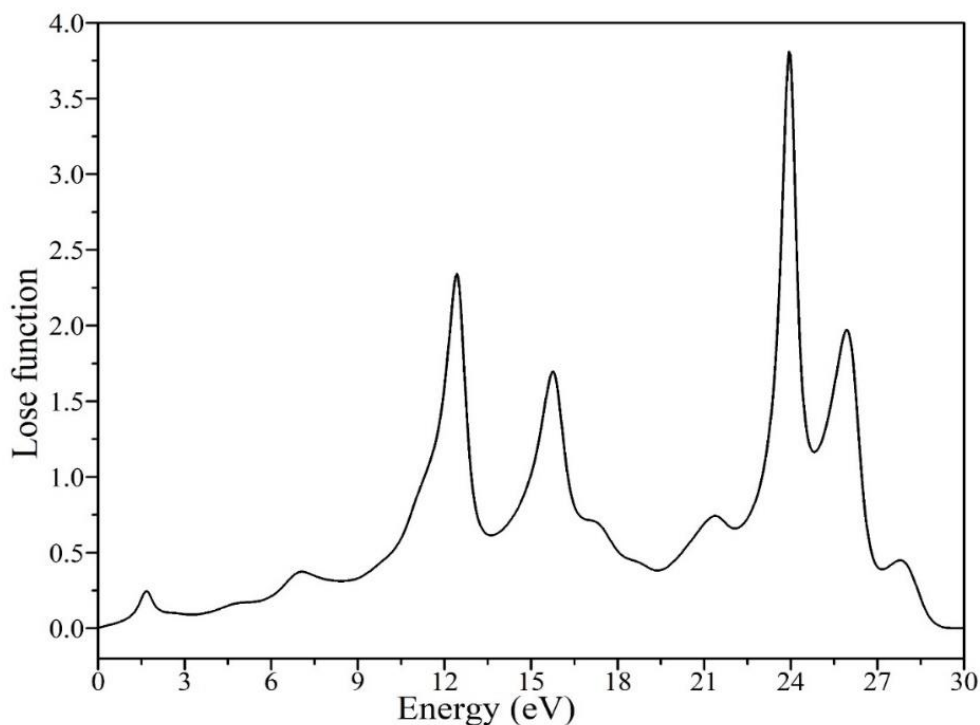


**Fig. 7.** delineates the refractive index and attenuation coefficient for the compound KCrS.



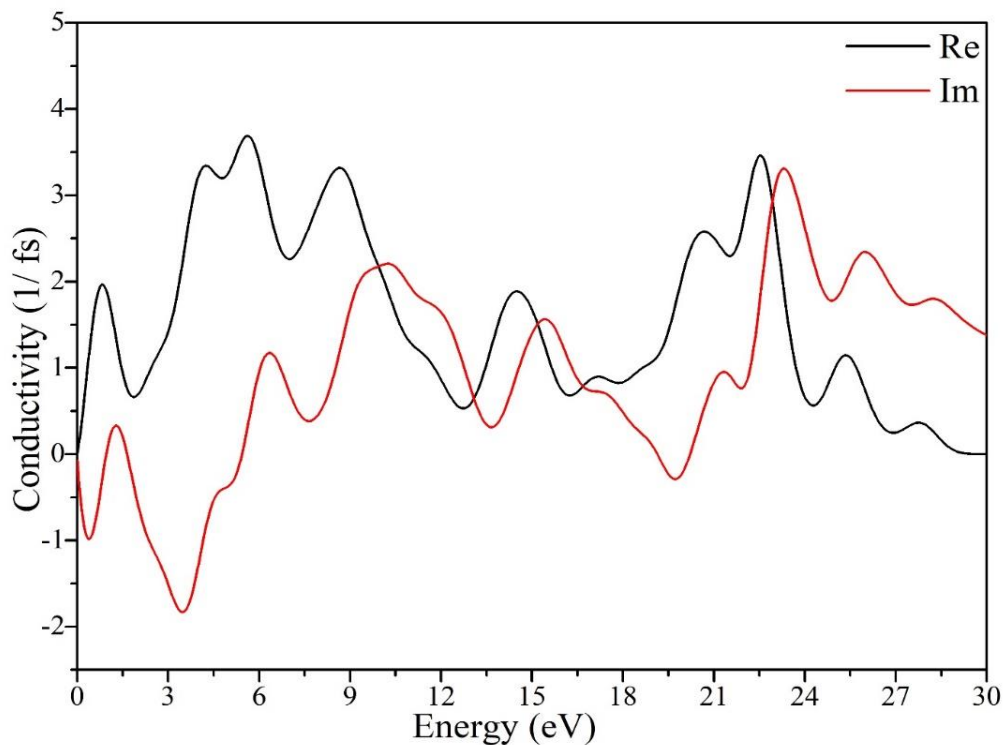
**Fig.8.** depicts the reflectivity of the KCrS compound.

Fig. 9 illustrates the loss function as a function of photon energy, where the loss function is nearly zero when the energy is zero. This signifies the absence of electronic transitions in this energy range. Notably, peaks are observed at photon energies (12.42 eV, 15.76 eV, 23.93 eV, and 25.92 eV), with the maximum peak occurring at 23.93 eV. These energies indicate the transition points from the metallic to insulating properties of the KCrS compound, suggesting its potential as an efficient absorber for the low to mid-range UV spectrum [29].



**Fig.9.** Loss Function Analysis for the compound KCrS.

Fig. 10 illustrates the optical conductivity as a function of energy. The real part of the conductivity for the KCrS compound exhibits a single peak in the infrared region, specifically at an energy of 0.83 eV. Meanwhile, several prominent peaks are observed in the ultraviolet region. On the other hand, the imaginary part of the conductivity also features a peak in the infrared region and multiple peaks in the ultraviolet region, with the most prominent one occurring at an energy of 23.32 eV. Seeing the negative imaginary values of the conductivity which are shown on the figure.



**Fig.10.** Photon Energy-Dependent Optical Conductivity in a Half-Heusler KCrS Compound.

#### 4. Conclusion

In our current study, a complete investigation about the structure, electrons and light aspects of the half-Heusler KCrS alloy has been carried out using first principles calculation method. Through making use of the full-potential-linearized-augmented-plane-wave (FP-LAPW) method in the DFT approach, we uncover (and discover) the unique features of this compound, and we show that it is structurally stable and has interesting magnetic and optical properties. Such a refined computational approach enables one to make even stronger credibility in the understand level of the character and prospect of the KCrS in real life. The results revealed that bulk KCrS belongs to the ferromagnetic half-metal category with a band gap of 3.29 eV and spin polarization of 100 % in the electron down-spin. The KCrS lattice constant of the KCrS alloy equals 6.63Å for its equilibrium point. In addition, the sum of the local magnetic moments in the KCrS compound is found to be 5 $\mu$ B. On the side of optical parameters, the FP-LPAW method is used to calculate several parameters including real and imaginary parts of the dielectric function, reflectivity, conductivity, optical absorption and loss function. This technique, which deals with band-to-band and band-to-band excitations, is considered to be the best one. Imaginary parts of the dielectric function through interband transition primarily become peaks. The graphic representation of the dielectric function as a function of energy as well as that of the reflectivity coefficient indicates that there is a metallic feature at extremely low energies. Moreover, there is also observed enlargement amount of light absorption due to the lowered transition rate of electrons at higher energy levels.

#### 5. References

- [1] B. E. Iyozzor and M. I. Babalola, "Half-metallic Characteristics of the Novel Half Heusler Alloys XCrSb (X=Ti, Zr, Hf)," *J. Nig. Soc. Phys. Sci.*, vol. 3, pp. 138-145, 2022. Doi:<https://doi.org/10.46481/jnsps.2022.297>
- [2] K. Nawa and Y. Miura, "Ab-initio Search for Half-Metallic Co-based Full Heusler Alloys: Linear-Response-Based DFT+ U Study," 2019. arXiv preprint arXiv:1903.00180.
- [3] S. Kämmerer, et al., "Co2MnSi Heusler alloy as magnetic electrodes in magnetic tunnel junctions," *Appl. Phys. Lett.*, vol. 85, no. 1, pp. 79-81, 2004. Doi:<https://doi.org/10.1063/1.1769082>
- [4] J. Winterlik, et al., "Design scheme of new tetragonal heusler compounds for spin-transfer torque applications and its experimental realization," *Adv. Mater.*, vol. 24, no. 47, pp. 6283-6287, 2012. Doi:<https://doi.org/10.1002/adma.201201879>
- [5] J. F. Gregg and P. D. Sparks, "Spin Transistor," U.S. Patent 6 294 785, Sep 25 2001.
- [6] G. Tanja, S. S. P. Parkin, and C. Felser, "Heusler Compounds—A Material Class with Exceptional Properties," *IEEE Trans. Magn.*, vol. 47, 2010. Doi:<https://doi.org/10.1109/TMAG.2010.2096229>
- [7] H. Atsufumi and K. Takanashi, "Future perspectives for spintronic devices," *J. Phys. D Appl. Phys.*, vol. 47, 2014. Available: <http://iopscience.iop.org/0022-3727/47/19/193001>
- [8] I. Galanakis, P. H. Dederichs, and N. Papanikolaou, "Slater-Pauling behavior and origin of the half-metallicity of the full-Heusler alloys," *Phys. Rev. B*, vol. 66, 2002. Doi:<https://doi.org/10.1103/PhysRevB.66.174429>
- [9] S. Sugahara and M. Tanaka, "A spin metal–oxide–semiconductor field-effect transistor using half-metallic-ferromagnet contacts for the source and drain," *Appl. Phys. Lett.*, vol. 84, pp. 2307-2309, 2004.
- [10] I. Muhammad, J.-M. Zhang, A. Ali, M. U. Rehman, and S. Muhammad, "First-principles prediction of the quaternary half-metallic ferromagnets TiZrIrZ (Z = Al, Ga or In) for spintronics applications," *Thin Solid Films*, vol. 690, 2019.

- Doi:<https://doi.org/10.1016/j.tsf.2019.137564>
- [11] F. Khelifaoui, M. Ameri, D. Bensaid, I. Ameri, and Y. Al-Douri, "Structural, elastic, thermodynamic, electronic, and magnetic investigations of full-Heusler compound  $\text{Ag}_2\text{CeAl}$ : FP-LAPW method," *J. Supercond. Nov. Magnetism*, vol. 31, pp. 3183-3192, 2018. Doi:<https://doi.org/10.1007/s10948-017-4530-6>
- [12] R. A. de Groot, F. M. Mueller, P. G. van Engen, and K. H. J. Buschow, "New class of materials: half-metallic ferromagnets," *Phys. Rev. Lett.*, vol. 50, pp. 2024-2027, 1983.
- [13] P. Cui, J. Zeng, H. Peng, J.-H. Choi, Z. Li, C. Zeng, C.-K. Shih, J. P. Perdew, and Z. Zhang, "Predictive design of intrinsic half-metallicity in zigzag tungsten dichalcogenide nanoribbons," *Phys. Rev. B*, vol. 100, 2019. Doi:<https://doi.org/10.1103/PhysRevB.100.195304>
- [14] Lorenzo Poggini, et al., "Vertical tunnel junction embedding a spin crossover molecular film," *Advanced Electronic Materials*, vol. 4, no. 12, 2018, 1800204. Doi:<https://doi.org/10.1088/13616501/aa902c>
- [15] Feifei Chen, et al., "Fiber optic refractive index and magnetic field sensors based on microhole-induced inline Mach-Zehnder interferometers," *Meas. Sci. Technol.*, vol. 29, no. 4, 2018, 045103. Doi:<https://doi.org/10.1088/1361-6501/aa902c>.
- [16] J. M. Khalaf Al-zyadi, G. Y. Gao, and K. L. Yao, "First-principle study of half-metallicity at the  $\text{TiPo}$  (001) surface and the  $\text{TiPo}/\text{CdTe}$  (001) interface," *Thin Solid Films*, vol. 531, pp. 266, 2013. Doi:<https://doi.org/10.1016/j.tsf.2013.01.050>
- [17] J. M. Khalaf Al-zyadi, A. A. Kadhim, and K. L. Yao, "Half-metallicity of the (001), (111) and (110) surfaces of  $\text{CoRuMnSi}$  and interface half-metallicity of  $\text{CoRuMnSi}/\text{CdS}$ ," *RSC Adv.*, vol. 8, pp. 25653, 2018.
- [18] J. M. Khalaf Al-zyadi, W. A. Abed, and A. H. Ati, "Bulk, surfaces, and interface investigations of electronic and magnetic properties: A case of the half-Heusler alloy  $\text{MgCaB}$ ," *Phys. Lett. A*, vol. 411, 2021. Doi:<https://doi.org/10.1016/j.physleta.2021.127572>
- [19] J. M. Khalaf Al-zyadi, G. Y. Gao, and K. L. Yao, "First-principles investigation of the structural and electronic properties of bulk full-Heusler alloy  $\text{Mn}_2\text{CoSn}$  and its (001) surface," *J. Alloys Compd.*, vol. 565, pp. 17, 2013. Doi:<https://doi.org/10.1016/j.jallcom.2013.02.181>
- [20] J. M. Khalaf Al-zyadi, H. I. Asker, and K. L. Yao, "The half-metallic properties of bulk and the (111), (110) and (001) surfaces for the full Heusler alloy  $\text{Zr}_2\text{VIn}$ ," *Phys. E Low-Dimens. Syst. Nanostruct.*, vol. 122, pp. 1, 2020. Doi:<https://doi.org/10.1016/j.physe.2020.114196>
- [21] A. R. Mishra and Snehanshu Pal, "First-principles calculations to investigate electronic structure and magnetic, mechanical and thermodynamic properties of d0 half-Heusler  $\text{LiXN}$  ( $X = \text{Na}, \text{K}, \text{Rb}$ ) alloys," *Solid State Sciences*, vol. 118, 2021. Doi:<https://doi.org/10.1016/j.solidstatesciences.2021.106633>
- [22] A. Telfah, S. S. Essaoud, H. Baaziz, Z. Charifi, A. M. Alsaad, M. J. A. Ahmad, R. Hergenröder, and R. Sabirianov, "Density Functional Theory Investigation of Physical Properties of  $\text{KCrZ}$  ( $Z = \text{S}, \text{Se}, \text{Te}$ ) Half-Heusler Alloys," *Phys. Status Solidi B*, 2021. Doi:<https://doi.org/10.1002/pssb.202100039>.
- [23] P. Dharmaraj, A. Amudhavalli, M. Manikandan, Rajeswara Palanichamy R, and K. Iyakutti, "Electronic structure, magnetic and thermodynamic properties of yttrium based half Heusler alloys  $\text{YXZ}$  ( $X = \text{Fe}, \text{Co}, \text{Cr}$ ;  $Z = \text{As}, \text{Sb}$ ): A first principles study," *Computational Condensed Matter*, vol. 34, 2023. Doi:<https://doi.org/10.1016/j.cocom.2022.e00776>.
- [24] J. M. Khalaf Al-zyadi, H. I. Asker, "A study half-metallic surfaces of the full-Heusler  $\text{Sc}_2\text{CrGe}$  compound and the interface of  $\text{Sc}_2\text{CrGe}/\text{InSb}$  (111)," *J. Electron Spectrosc. Relat Phenom.*, vol. 249, 2021. Doi:<https://doi.org/10.1016/j.elspec.2021.147060>
- [25] R. Prakash, G. Kalpana, "First-principles study on novel Fe-based quaternary Heusler alloys,

- with robust half-metallic, thermoelectric and optical properties," *RSC Adv.*, vol. 13, pp. 10847, 2023.
- [26] A. Anjami, A. Boochani, S. M. Elahi, H. Akbari, "Ab-initio study of mechanical, half-metallic and optical properties of  $Mn_2ZrX$  ( $X = Ge, Si$ ) compounds," *Results in Physics*, vol. 7, pp. 3522–3529, 2017. Doi:<https://doi.org/10.1016/j.rinp.2017.09.008>.
- [27] A. A. Nasser, J. M. AL-Zyadi, "Investigate the electrical structure, optical characteristics, and phonon transport of the rock-salt (RS) CrTe monolayer using first-principles methods," *J. Basrah Res. (Sci.)*, vol. 49(1), pp. 57, 2023. Doi:<https://doi.org/10.56714/bjrs.49.1.6>
- [28] F. Mostari, Md. A. Rahman, R. Khatun, "First Principles Study on the Structural, Elastic, Electronic and Optical Properties of Cubic 'Half-Heusler' Alloy RuVAs Under Pressure," *Int. J. Mat. Math. Sci.*, vol. 2(4), pp. 51-63, 2020. Doi:<https://doi.org/10.34104/ijmms.020.051063>
- [29] M. Ahmad, Naeemullah, G. Murtaza, R. Khenata, S. Bin Omran, A. Bouhemadou, "Structural, elastic, electronic, magnetic and optical properties of RbSrX (C, SI, Ge) half-Heusler compounds," *J. Magn. Magn. Mater.*, vol. 377, pp. 204–210, 2015. Doi:<http://dx.doi.org/10.1016/j.jmmm.2014.10.108>

# دراسة التركيب الالكتروني والخصائص المغناطيسية والبصرية لمركب نصف هيوسلر KCrS من حسابات المبادئ الاولى

رباب عبد الرحمن صالح، جبار خلف منصور\*

قسم الفيزياء، كلية التربية للعلوم الصرفة، جامعة البصرة، العراق.

المعلومات البحث	المخلص
الاستلام القبول النشر	21 اذار 2024 23 ايار 2024 30 حزيران 2024
الكلمات المفتاحية	باستخدام المبادئ الأولية، التي أجريت في إطار نظرية الكثافة الوظيفية (DFT) وتقريب التدرج المعمم باستخدام برنامج WEN2K code. من أجل حساب الخصائص التركيبية والالكترونية والمغناطيسية والبصرية لمركب KCrS، أظهرت النتائج ان المركب يحقق خاصية نصف المعدن عند ثابت اتران الشبكة (6.63)، حيث يسلك سلوك المعدن في قناة البرم للأعلى بينما يتصرف كشبه موصل في قناة البرم للأسفل. اجمالي العزم المغناطيسي هو $5\mu_B$ . وفجوة الطاقة الكلية لهذا المركب هي (3.29 eV)، بالإضافة الى ذلك أظهر خصائص بصرية مميزة، مما يجعله خياراً ممتازاً للاستخدامات البصرية والكهروبصرية. هذه الخصائص الفريدة تبرز إمكانيات المركب في إنتاج انعكاس عالي في مناطق الأشعة فوق البنفسجية مما يجعله مرشحاً جذاباً في تقنية الليزر والانبعثات المحفز.
الكلمات المفتاحية	مركب نصف هيوسلر KCrS، نظرية الكثافة الوظيفية، نصف المعدن، العزم المغناطيسي.

Citation: R. A. Saleh, J. M. AL-Zyadi, J. Basrah Res. (Sci.) 50(1), 125 (2024).  
DOI: <https://doi.org/10.56714/bjrs.50.1.11>

\*Corresponding author email : jabbar.khalaf@uobasrah.edu.iq

